TECHNICAL REPORT R-95

SHIELDING OF PARTIALLY REFLECTING STAGNATION SURFACES AGAINST RADIATION BY TRANSPIRATION OF AN ABSORBING GAS

By JOHN THOMAS HOWE

Ames Research Center
Moffett Field, Calif.

TECHNICAL REPORT R-95

SHIELDING OF PARTIALLY REFLECTING STAGNATION SURFACES AGAINST RADIATION BY TRANSPIRATION OF AN ABSORBING GAS

By JOHN THOMAS HOWE

SUMMARY

The laminar compressible boundary layer for two-dimensional and axisymmetric stagnation regions has been analyzed to show the effects of the injection of a radiation absorbing gas on the incident radiation field, on enthalpy profiles, and on heat transfer to the vehicle surface. It is assumed that the energy emitted from the cold foreign gas is negligible compared with that absorbed. It is shown that the reduction of radiation heat-transfer rate to the surface by radiation absorption in the injected gas is accompanied by an increase in the convective heat-transfer rate. For a black surface, a saving in total heat transfer is achieved by injection of an absorbing gas. On the other hand, for a totally reflecting surface, it is not desirable to inject an absorbing gas because the total heat transfer is increased. The reflectivity condition between the totally reflecting and the black surface extremes below which it is desirable to inject an absorbing gas is determined. Heat-transfer results are presented and are compared with those of the unshielded case. The required absorption properties of the foreign gas are determined and compared with absorption properties of known gases.

INTRODUCTION

In some regimes of high-speed flight, particularly during entry into planetary atmospheres at speeds greater than circular orbit speed, the shock layer on a blunt body emits thermal radiation which is incident on the surface of the vehicle. The radiant flux becomes more intense with increasing flight speed, diminishing altitude, and increasing body nose radius. Kivel (ref. 1) analyzes the radiation heat transfer from the inviscid equilibrium shock layer to the stagnation point. His results show, for example, that the radiation heat transferred to the stagnation region exceeds the convective heat transferred if the nose radius of curvature is greater than about 1.7 feet and the vehicle is traveling at 36,700 ft/sec (escape speed) at 200,000 feet altitude. If the shock layer air is not in chemical equilibrium, the radiant heating may be greater than that shown by Kivel for equilibrium air.

The problem of shielding the vehicle surface from this thermal radiation becomes important. It is well known (ref. 2) that convective heating in the stagnation region can be greatly diminished by the injection of gas into the boundary layer. The possibility exists that the radiative heat transferred to the vehicle surface can also be diminished if the gas injected (by transpiration or ablation) into the boundary layer absorbs radiation. Of course, the absorption of radiation by the injected gas raises the gas temperature and thus the temperature gradient of the boundary layer at the wall, and therefore increases the convective heat transferred to the vehicle. The question arises as to whether or not a net saving of total heat transfer (convective plus radiative) can be achieved by injection of an absorbing gas, and if so, what gas properties are necessary to reduce the total heat transfer effectively.

An exploratory analysis (ref. 3) in which the boundary layer was assumed to be a binary mixture of undissociated air and inert foreign gas and the vehicle surface was assumed to be completely absorbing yielded encouraging results. It was shown that injection of an absorbing gas through the black surface into the boundary layer yields a substantial saving in total heat transfer. However, if the vehicle surface were totally reflecting, it would not be desirable to inject an absorbing gas into the boundary layer because, although there would be no radiative heat transfer to the totally reflecting surface, the convective heat-transfer rate

would be increased by the absorption of radiant energy in the foreign gas near the vehicle surface.

Actual surfaces are neither completely absorbing nor totally reflecting. Somewhere between these two extremes is a reflectivity above which the total heat-transfer rate is increased and below which it is diminished by injection of an absorbing gas. This "break even" reflectivity is important because above it the injected gas should be nonabsorbing and below it the injected gas should be absorbing in order to diminish total aerodynamic heating.

The purpose of this paper is to study the effects of an absorbing gas injected into the boundary layer on the combination of convective and radiative heat transfer to partially reflecting stagnation surfaces of bluff bodies traveling at hypersonic speed. In this paper, many of the results of reference 3 are retained as well as the simplifying assumption that the energy emitted by the foreign gas is small compared with the energy absorbed. The results of that analysis as well as of the present paper are made applicable to a mixture of air in chemical equilibrium and an inert foreign species. The present paper goes on to analyze the case of the partially reflecting wall, and to account for the reflected radiant energy. The heat transfer is evaluated and the break-even reflectivity is determined as a function of the absorption coefficient of the foreign gas.

It is pointed out that an exact analysis of the interaction of a radiation field with a mixture of dissociated air and a foreign gas in the compressible laminar boundary layer is a very difficult problem because it requires the solution of a set of nonlinear, coupled, partial-differential integral equations, such as those formulated in reference 4. For this reason, simplifying assumptions are made which make the problem more tractable. It is expected that the results of the analysis retain significant aspects of the actual physical behavior.

SYMBOLS

a slope of lines in figure 5 and equation (48)

c_p specific heat at constant pressure

$\bar{c}_p$ defined by equation (10)

C Chapman-Rubesin function, $\frac{\rho\mu}{\rho_e\mu_e}$

D coefficient of diffusion

f, F dimensionless stream functions

$\vec{F}$ radiation flux

g ratio of total enthalpy to total enthalpy exterior to the boundary layer

h static enthalpy of the mixture

$h_m°$ heat of formation of the mth species at 0° K

I radiation intensity (integrated over wavelength)

I_i magnitude of intensity of incident radiation beam

I_r magnitude of intensity of reflected radiation beam

j total enthalpy, $h+\frac{u^2}{2}$

k thermal conductivity

K absorption coefficient, defined by equations (13) and (14)

l dimensionless radiation intensity defined by equation (30)

Le Lewis number, $\frac{\overline{Pr}}{Sc}$

n exponent in equation (1), zero for two-dimensional case and unity for axisymmetric case

p pressure

P_m mass rate of production of the mth species per unit volume

$Pr, \overline{Pr}$ Prandtl number, $\frac{c_p\mu}{k}$ and $\frac{\bar{c}_p\mu}{k}$

q total heat-transfer rate (convective and radiative)

r surface reflectivity

r^* break-even surface reflectivity

r_o radius of cross section of body of revolution

s transformed independent variable parallel to body surface (eq. (18))

Sc Schmidt number, $\frac{\mu}{\rho D}$

T temperature

U_∞ velocity of the free stream ahead of the bow shock

u velocity component parallel to surface

v velocity component normal to surface

W mass fraction of foreign absorbing gas

W_m mass fraction of species m, $\frac{\rho_m}{\rho}$

x distance along body surface from the stagnation point

y	distance normal to body surface
α	dimensionless gas absorption coefficient defined by equation (36)
β	constant in velocity relationship (eq. (26))
η	dimensionless transformed independent variable normal to body surface (eq. (19))
μ	coefficient of viscosity
ρ	gas density
ψ	stream function
ξ	$\frac{\eta}{\sqrt{2}}$

SUPERSCRIPTS

$'$,$''$,$'''$	derivatives with respect to the independent variable concerned

SUBSCRIPTS

e	properties evaluated at the outer edge of the boundary layer
i	radiation incident on body
m	properties of the mth species
r	radiation reflected from body
w	properties evaluated at the wall
1	foreign absorbing gas in the boundary layer
2	air
$\alpha=0$	properties of a nonabsorbing gas and air
$f_w=0$	no injection case: all air boundary layer
$I_{ie}=0$	mixture of absorbing gas and air with no incident radiation

ANALYSIS

The physical model chosen for analysis is represented by sketch (a). The region between the bow shock and the body surface is divided into an inviscid shock layer of hot radiating air, and a boundary layer consisting of a mixture of air and a foreign absorbing gas being injected through and normal to the porous body surface.

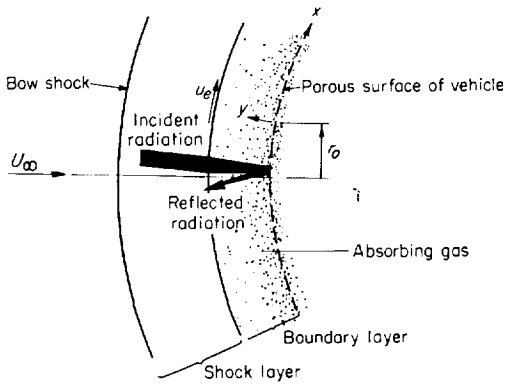

Sketch (a)

The following assumptions are made regarding the properties of these regions. Additional assumptions will appear and be discussed where they are needed in the analysis.

1. The radiant energy is incident on the outer edge of the boundary layer in beams of radiation with integrated (over wavelength) intensity of magnitude I_{ie} (ref. 5, eq. (5)), all assumed to be traveling normal to the wall. Although I is often defined as the intensity for unit solid angle, it is considered here to be intensity per unit differential thickness of these parallel rays in the manner of reference 6, page 53. Thus, I is equivalent to the y component of the flux of radiant energy.

2. The air within the boundary layer is assumed to be transparent to the incident radiation, and its emitted radiation is neglected in comparison with the incident radiation.

3. The injected foreign gas, which will absorb a portion of the incident radiation before it reaches the body surface, has absorption properties which are assumed to be independent of the wavelength of the radiation (i.e., it is a gray gas).

4. The surface of the vehicle is assumed to be cold and to emit no radiation.

Because of a general lack of knowledge of the radiation properties of gases, it is advantageous to specify various properties of the foreign absorbing gas and otherwise keep the analysis as general as possible. In this way, the gas properties necessary to achieve a reduction of heat transfer can be determined, after which one is in a position to ask if a gas having these radiation properties exists.

The partial differential equations describing the laminar compressible boundary layer of a mixture of gases (ref. 7) in the presence of a radiation field are statements of continuity, the momentum theorem, conservation of energy, and diffusion of species. The first two are expressed, respectively, as:

$$\frac{\partial}{\partial x}(\rho u r_o^n)+\frac{\partial}{\partial y}(\rho v r_o^n)=0 \tag{1}$$

$$\rho u\left(\frac{\partial u}{\partial x}\right)+\rho v\left(\frac{\partial u}{\partial y}\right)=\frac{\partial}{\partial y}\left(\mu\frac{\partial u}{\partial y}\right)-\frac{\partial p}{\partial x} \tag{2}$$

Two exactly equivalent forms of the energy equations are listed and will be used subsequently to illustrate the applicability of the solutions to either a binary mixture of undissociated air and an inert foreign species or a binary mixture of air in chemical equilibrium and an inert foreign species. The two energy equations written below differ only in form; the differences arise from the definitions of Pr and $\overline{Pr}$.

$$\rho u\frac{\partial j}{\partial x}+\rho v\frac{\partial j}{\partial y}=\frac{\partial}{\partial y}\left(\frac{\mu}{Pr}\frac{\partial j}{\partial y}\right)+\frac{\partial}{\partial y}\left[\mu\left(1-\frac{1}{Pr}\right)\frac{\partial u^2/2}{\partial y}\right]+\frac{\partial}{\partial y}\left(\rho D\sum h_m\frac{\partial W_m}{\partial y}\right)-\operatorname{div}\vec{F} \tag{3a}$$

or

$$\rho u\frac{\partial j}{\partial x}+\rho v\frac{\partial j}{\partial y}=\frac{\partial}{\partial y}\left(\frac{\mu}{\overline{Pr}}\frac{\partial j}{\partial y}\right)+\frac{\partial}{\partial y}\left[\mu\left(1-\frac{1}{\overline{Pr}}\right)\frac{\partial u^2/2}{\partial y}\right]+\frac{\partial}{\partial y}\left[\rho D\left(1-\frac{1}{Le}\right)\sum h_m\frac{\partial W_m}{\partial y}\right]-\operatorname{div}\vec{F} \tag{3b}$$

The diffusion equation, written for the mth species, is

$$\rho u\frac{\partial W_m}{\partial x}+\rho v\frac{\partial W_m}{\partial y}-\frac{\partial}{\partial y}\left(\rho D\frac{\partial W_m}{\partial y}\right)=P_m \tag{4}$$

We will only need this equation for the inert foreign species (for which $P_m=0$), so hereafter, for this equation we drop the subscript m and note that W is the mass fraction of the inert foreign species. The boundary conditions for equations (1) through (4) are

at $y=0$

$$v=v_w,\ u=0,\ j=j_w,\ W=W_w \tag{5}$$

at $y\to\infty$

$$u\to u_e,\ j\to j_e,\ W\to 0 \tag{6}$$

A few relationships for enthalpy and heat transfer are needed.

The enthalpy of the mixture is defined as

$$h=\Sigma\, W_m h_m \tag{7}$$

where

$$h_m=\int_0^T c_{p_m}dT+h_m^\circ \tag{8}$$

The specific heat at constant pressure is

$$c_p=\left(\frac{\partial h}{\partial T}\right)_p=\sum\left[W_m\left(\frac{\partial h_m}{\partial T}\right)_p+h_m\left(\frac{\partial W_m}{\partial T}\right)_p\right]$$

or

$$c_p=\bar{c}_p+\sum h_m\left(\frac{\partial W_m}{\partial T}\right)_p \tag{9}$$

where

$$\bar{c}_p=\sum W_m\left(\frac{\partial h_m}{\partial T}\right)_p=\sum W_m c_{p_m} \tag{10}$$

The heat-transfer rate at the wall due to convection, diffusion, and radiation is:

$$q_w=-\left[k\frac{\partial T}{\partial y}+\rho D\sum\left(h_m\frac{\partial W_m}{\partial y}\right)+(1-r)I_i\right]_w \tag{11}$$

This can be rewritten as

$$q_w=-\left(\frac{\mu}{\overline{Pr}}\right)_w\left[\frac{\partial j}{\partial y}+(Le-1)\sum h_m\frac{\partial W_m}{\partial y}\right]_w-(1-r)I_{iw} \tag{12}$$

First, consider a binary mixture of undissociated air and an inert foreign gas for which h_m° (the heat of formation) is zero. If at every temperature $c_{p_2}=c_{p_1}$ (which was assumed in ref. 3), then $h_2=h_1$ from equation (8), $c_p=\overline{c_p}$ from equation (9), and $Pr=\overline{Pr}$. The third term on the right-hand sides of equations (3a) and (3b) vanishes, and the forms of the equations (and their solutions) are identical.

Secondly, consider a mixture of dissociated air in chemical equilibrium and an inert foreign gas. For the purposes of this paper, this mixture is considered to be a binary mixture. The inert foreign species is associated with either the air atoms or the air molecules, depending on which of these its molecular weight and mutual collision cross section matches best (ref. 7, p. M6). The energy equation in the form (3b) is used and the third term on the right-hand side is omitted by assuming $Le=1$. For the same boundary conditions and for a given $\overline{Pr}$, the solutions of (3b) under these conditions are identical with those of the undissociated mixture (where equation (3a) was used and the specific heats were considered equal). The heat transfer is also identical because the middle (diffusion) term on the right-hand sides of equations (11) and (12) vanishes.

In reference 3, the case of equal specific heats was studied. The value of Pr (or $\overline{Pr}$) was 0.72. However, from the preceding discussion it is seen that the results of that reference as well as those

of the present paper are applicable to the mixture of equilibrium air and foreign species where $Le=1$, $\overline{Pr}=0.72$, and it is not necessary that the specific heats be equal.

The last term in the energy equation (3) is the rate of gain of energy per unit volume due to the interaction of the radiation flux with the matter in the element volume. For the general case where the element of gas volume is exchanging radiant energy (by absorption and emission) with all other elementary gas volumes inside and outside the boundary layer, the radiation flux is expressed by integration over all space. Then the energy equation (3) is a partial-differential integral equation which is exceedingly difficult to solve. As mentioned previously, the problem will be simplified by neglecting the radiant energy emitted by the absorbing gas in comparison with the radiant energy absorbed. An energy balance is still maintained, of course; enthalpy and other forms of energy are simply not diminished by emission of radiation.

The simplification is justifiable if the rate of energy emission from the foreign gas is small compared with the rate of absorption. This situation can be realized under the following circumstances. It can be expected a priori that a large mass fraction of the cold dense boundary-layer region (near the wall) will be absorbing gas, but only a small mass fraction of the hot, much less dense region (away from the wall) will be absorbing gas. Therefore, the bulk of the absorbing gas is in the dense region which is cold compared with the shock layer. If the shock layer and boundary layer are behaving like black bodies and because they both emit energy at a rate proportional to the fourth power of their respective temperatures, then it is possible that the energy emitted by the shock layer (and thus absorbed by the foreign gas) is large compared with energy emitted by the boundary layer, and the latter may be neglected.

Until a better understanding of the energy emitted from the shock layer is achieved, it is not possible to say if or when the above assumption is strictly valid for flight conditions. It can of course be valid under laboratory conditions where the radiant energy is emitted from an external high temperature source. At any rate, by studying this extreme of the problem, it is possible to gain some insight into the more general problem. Suffice it to say that in the present analysis, the radiant energy emitted by the absorbing gas is neglected in favor of the energy absorbed, and the results apply when that situation exists.

In order to express the last term in equation (3b), we consider the radiation intensity in the y direction, and account for both the beam incident on the boundary layer and its subsequent reflection from the wall. For either the incident or reflected beam, the fraction of the local intensity absorbed in traveling a small distance is proportional to the local density of the absorbing gas, and to the small distance. Thus, following the form of reference 8 (pp. 5 and 24), for a fixed x and the incident beam traveling in the negative y direction (toward the wall)

$$\frac{\partial I_i}{\partial y}=K\rho_1 I_i \tag{13}$$

and similarly for the reflected beam traveling in the positive y direction

$$\frac{\partial I_r}{\partial y}=-K\rho_1 I_r \tag{14}$$

where K is the absorption coefficient and the intensity I in the positive y direction is defined as the difference of the reflected and incident intensities

$$I=I_r-I_i \tag{15}$$

where positive numbers will be used for both I_i and I_r (which are magnitudes only). Because we have assumed that there is no scattering and have neglected emission in the boundary layer, there is only a y component of the radiative flux and thus the last term in the energy equation (3b) is simply

$$\text{div } \vec{F}=\frac{\partial I_r}{\partial y}-\frac{\partial I_i}{\partial y} \tag{16}$$

which is evaluated by means of equations (13) and (14). The corresponding boundary conditions, evaluated at the wall as a matter of convenience, are

at $y=0$

$$\left.\begin{aligned} I_i&=I_{iw}\\ I_r&=I_{rw}=rI_{iw}\\ \text{and, or course,}&\\ I&=I_{iw}(r-1)\end{aligned}\right\} \tag{17}$$

The Levy transformation (ref. 9), a stream function, several definitions and assumptions, and some exterior flow relationships are to be used now to transform equations (1), (2), (3b), (4), (13), and (14) from x and y as independent variables to s and η, as follows:

The Levy transformation is

$$s=\int_0^x \rho_e u_e \mu_e r_0^{2n} dx \tag{18}$$

$$\eta=\frac{u_e r_0^n}{\sqrt{2sC}}\int_0^y \rho dy \tag{19}$$

A stream function is defined so that

$$\frac{\partial \psi}{\partial y}=\rho u r_0^n, \quad -\frac{\partial \psi}{\partial x}=\rho v r_0^n \tag{20}$$

and the continuity equation (1) is satisfied. The following quantities are defined

$$g(\eta)=\frac{j}{j_e} \tag{21}$$

$$\frac{\rho\mu}{\rho_e\mu_e}=C \quad \text{(ref. 10)} \tag{22}$$

where C is assumed constant and

$$f'(\eta)=\frac{u}{u_e} \tag{23}$$

from which

$$f(\eta)=\frac{\psi}{\sqrt{2sC}} \tag{24}$$

In the axisymmetric blunt body stagnation region it is assumed that

$$r_0=x \tag{25}$$

At the outer edge of the boundary layer, the velocity is described by

$$u_e=\beta x \tag{26}$$

and it is assumed that

$$\rho_e\mu_e=(\rho_e\mu_e)_{\text{stagnation}} \tag{27}$$

Use of equations (25), (26), and (27) in equations (18) and (19) yields

$$s=\frac{\beta\rho_e\mu_e x^{2(n+1)}}{2(n+1)} \tag{28}$$

$$\eta=\sqrt{\frac{(n+1)\beta}{C\rho_e\mu_e}}\int_0^y \rho\, dy \tag{29}$$

Thus for two-dimensional and axisymmetric flows, s is proportional to x^2 and x^4, respectively, while η is a function of y weighted by the density variation. A dimensionless radiation flux is defined by

$$l(\eta)=\frac{I}{j_e\rho_e u_e\mu_e r_0^n}\sqrt{\frac{2s}{C}} \tag{30}$$

Formally transforming equations (2), (3b), (4), (13), and (14) to the new independent variables s and η by means of the newly defined quantities and the assumptions results in the following set of differential equations (with constant Pr and Sc)

$$f'''+ff''=\frac{2s}{u_e}\left(\frac{du_e}{ds}\right)\left(f'^2-\frac{\rho_e}{\rho}\right) \tag{31}$$

$$\frac{1}{Pr}g''+fg'-l'=-\frac{u_e^2}{je}\frac{\partial}{\partial\eta}\left[\left(1-\frac{1}{Pr}\right)f'f''\right] \tag{32}$$

$$fW'+\frac{1}{Sc}W''=0 \tag{33}$$

$$l_i'-\alpha W l_i=0 \tag{34}$$

$$l_r'+\alpha W l_r=0 \tag{35}$$

where W is now the local mass fraction of the foreign absorbing gas and is assumed to be a function of η alone, and

$$\alpha=K\sqrt{\frac{\rho_e\mu_e C}{(n+1)\beta}} \tag{36}$$

The l' in equation (32) is expressed by transforming equation (16) and combining with equations (34) and (35).

$$l'=-\alpha W(l_i+l_r) \tag{37}$$

The boundary conditions (5), (6), and (17) transform to:

at $\eta=0$

$$\left.\begin{aligned} f=f_w, \quad f'=0, \quad g_w=0, \quad W=W_w \\ l_i=l_{iw}, \quad l_r=l_{rw}=rl_{iw} \end{aligned}\right\} \tag{38}$$

at $\eta\to\infty$

$$f'\to 1, \quad g\to 1, \quad W\to 0 \tag{39}$$

where f_w is proportional to the rate of injection of the absorbing gas (as will be shown subsequently) and the third of conditions (38) comes from the facts that the wall is much colder than the flow at the outer edge of the boundary layer and the air is assumed to be in chemical equilibrium.

The right-hand side of equation (31) will be neglected by virtue of the qualitative physical argument of reference 11 (based on the fact that the surface temperature is much lower than T_e). Equation (31) with the right-hand side equal to zero is the familiar Blasius equation (ref. 12) where η is related to the Blasius ξ, and $f(\eta)$ and its derivatives are related to the Blasius $F(\xi)$ and its derivatives by

$$\left.\begin{aligned} \eta&=\sqrt{2}\xi \\ f(\eta)&=\frac{F(\xi)}{\sqrt{2}} \\ f'(\eta)&=\frac{F'(\xi)}{2} \\ f''(\eta)&=\frac{F''(\xi)}{2\sqrt{2}} \end{aligned}\right\} \tag{40}$$

Equations (40) cause the boundary conditions of $f(\eta)$ to be compatible with the boundary conditions on $F(\xi)$ and with the values of reference 13. A solution of equation (31) with the right-hand side equal to zero can be obtained at once from reference 13.

Next, the right-hand side of equation (32) will be neglected because $u_e^2 \ll j_e$ for the stagnation region in hypersonic flow. Thus the similarity solutions of equations (33), (34), (35), and

$$f'''+ff''=0 \tag{41}$$

$$\frac{1}{Pr}g''+fg'-l'=0 \tag{42}$$

subject to boundary conditions (38) and (39), will be sought in which all dependent variables are a function of one independent variable η.

The boundary conditions (38) and (39) on the diffusion equation are mathematically sufficient, but are not very useful for initiating the numerical integration at $\eta=0$. For this reason, it is necessary to choose initial values of W_w and W_w' so that (1) a mass balance of the air at the surface is satisfied for a given injection rate, and (2) $W(\infty)\to 0$. The assumption that there is no net penetration of air into the wall through which the absorbing gas is injected leads to the following mass balance of the air at the wall (where the first term corresponds to the mass rate of molecular diffusion of air and the second term to the mass rate of flow of air)

$$\rho_w D_w\left(\frac{\partial W}{\partial y}\right)_w+\rho_w v_w(1-W_w)=0 \tag{43}$$

which when transformed to the independent variable η becomes

$$W_w'=Scf_w(1-W_w) \tag{44}$$

Formally integrating equation (33) twice, making use of equation (41), the boundary conditions (38) and (39), and equation (44) leads to

$$W_w=\frac{1}{1-\left[(f_w'')^{Sc}/f_wSc\int_0^\infty (f'')^{Sc}d\eta\right]} \tag{45}$$

Equation (45) gives the value of W_w which imposes the condition that $W(\infty)\to 0$. Equation (44) gives the corresponding W_w' used to begin the numerical integration of equation (33).

In the radiation absorption law (eqs. (34) and (35)), the absorption coefficient α (and therefore K) is assumed to be constant, although in principle, K could be any function of η and would thus comply with the similarity requirement.

METHOD OF SOLUTION

Equations (41), (42), (33), (34), and (35) subject to boundary conditions (38) and (39) were integrated numerically by the Adams-Moulton (ref. 14, p. 200, eqs. 6.6.2) predictor corrector method using the IBM 704 electronic data processing machine. Briefly, the sequence of machine computation was as follows: the quantities f_w, f_w', f_w'', g_w, l_w, Pr, Sc, and α are specified (f_w and f_w'' are obtained from reference 13 by use of equations (40)). Equation (41) was integrated numerically as a convenience for the machine computation and simultaneously the integral $\int_0^\infty (f'')^{Sc}d\eta$ was evaluated for use in equation (45). Initial values W_w and W_w' were obtained from equations (45) and (44), respectively. Two

values of g_w' were arbitrarily chosen. Each value of g_w' was used separately to integrate equation (42). The values of $g(\infty)$ resulting from the two integrations were used to interpolate linearly to give an improved value of g_w' so that $g(\infty)=1$. The integration was repeated until the boundary conditions were satisfied. In all the numerical examples $\overline{Pr}$ is 0.72, Le is unity, and therefore Sc must be 0.72.

DISCUSSION OF RESULTS

From the solutions of the differential equations (41), (42), (33), (34), and (35), we first want to examine some features of the solutions- in particular, the mass distribution of the foreign species across the boundary layer and its effect (through the absorption coefficient) on radiation intensity at the wall, on the radiation intensity profiles, and on enthalpy profiles across the boundary layer. Then attention is directed to a heat-transfer evaluation for partially reflecting surfaces leading to the determination of the break even reflectivity condition mentioned previously.

Because most of the results are presented for specific injection rates, it is pertinent that the presentation be prefaced with a brief comment on injection rate. The symbol f_w is the value of the stream function at the wall and can be shown to be directly proportional to the mass injection rate by virtue of equations (20), (24), (18), (19), and (28) which are combined to yield

$$\rho_w v_w=-f_w\left(\rho_e u_e \mu_e r_o^n\sqrt{\frac{C'}{2s}}\right)=-f_w\sqrt{\beta C \rho_e \mu_e(\eta+1)} \tag{46}$$

An injection rate corresponding to $f_w=-1.283/\sqrt{2}$ leads at once to laminar separation (ref. 14 and eqs. (40)). The solutions in this paper were obtained for two injection rates; a strong rate corresponding to the near "blow-off" condition of $f_w=-1/\sqrt{2}$ and a weaker rate corresponding to $f_w=-1/2\sqrt{2}$.

FEATURES OF THE SOLUTIONS

For a specified value of f_w, there is one solution to the momentum equation (41). For this specified injection rate and a given Sc, there is one solution of the diffusion equation (33) and thus one profile of mass fraction of the foreign absorbing gas across the boundary layer. Figure 1

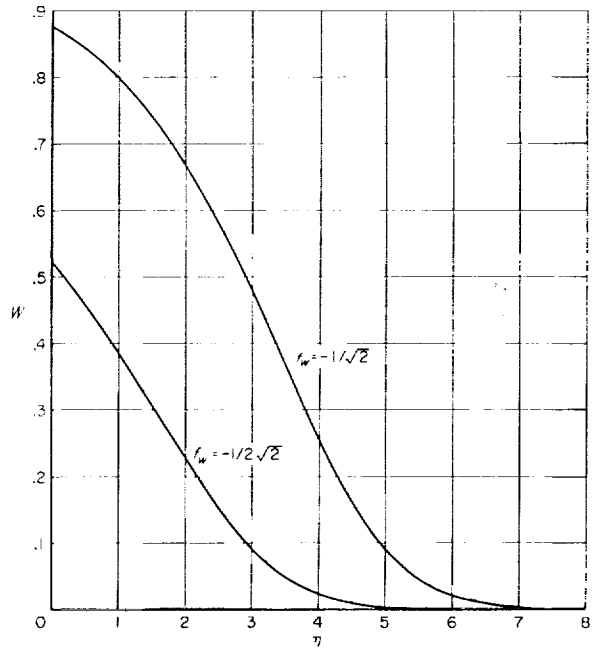

FIGURE 1. The mass fraction of the foreign absorbing gas as a function of the dimensionless distance from the surface for two injection rates; $Sc=0.72$.

shows two such concentration profiles corresponding to the two injection rates mentioned above. The ordinate W is the fraction of the local density that is due to the foreign gas. It is evident as was mentioned in the analysis that near the surface (small η), a large fraction of the density (which is also large) is foreign gas, whereas away from the surface (larger η), a small fraction of the density (which is also small) is foreign gas. Thus it is evident that the bulk of the mass of the foreign gas is in the more dense (and therefore the cold) region of the boundary layer.

Having these profiles of foreign gas concentration, we next inquire as to their effectiveness in shielding the surface from the incident radiation. The fraction of the incident radiation intensity which strikes the surface is shown in figure 2 as a function of the absorption coefficient α. The equation for the two curves shown in the figure is obtained by separating variables and integrating equation (34) which yields

$$\frac{I_{iw}}{I_{ie}}=e^{-\alpha\int_0^\infty W d\eta} \tag{47}$$

The integral $\int_0^\infty W d\eta$ has the values 2.73 and 0.968 for $f_w=-1/\sqrt{2}$ and $-1/2\sqrt{2}$, respectively.

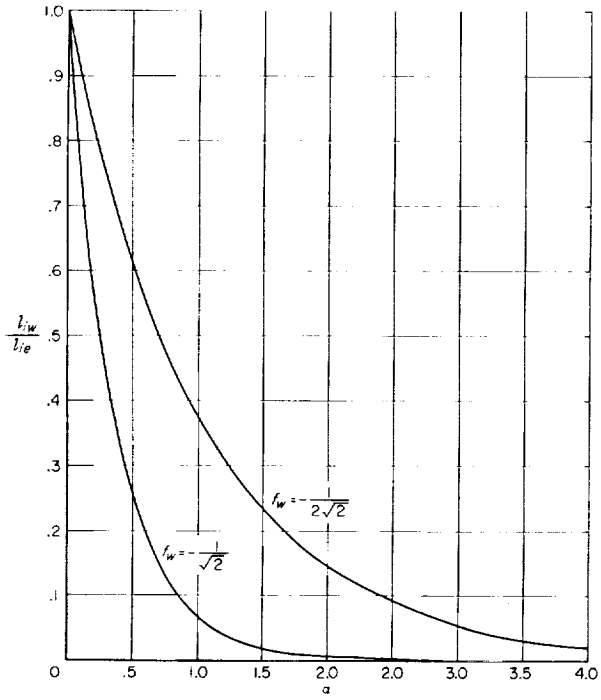

FIGURE 2.—The fraction of the incident radiation striking the surface as a function of the dimensionless gas absorption coefficient for two injection rates; $Sc=0.72$.

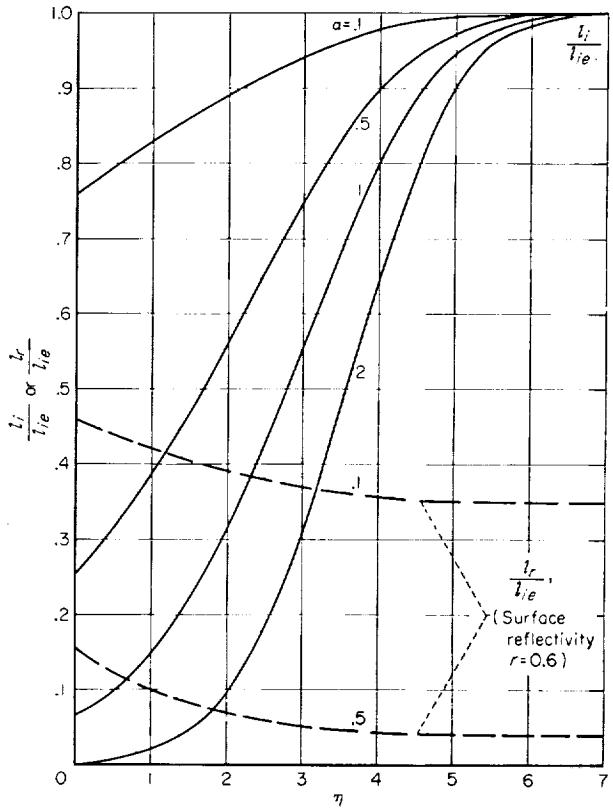

FIGURE 3.—Relative intensity of incident and reflected radiation as a function of the dimensionless distance from the surface for several values of dimensionless gas absorption coefficient; $f_w=-1/\sqrt{2}$, $Sc=0.72$.

It is observed that for a given value of the absorption coefficient α for the higher injection rate ($f_w=-1/\sqrt{2}$), much more radiation is absorbed in the boundary layer. It can be noted that if α is about 2 or greater, almost none of the incident radiation reaches the surface.

It is interesting to examine in detail how the radiation intensity diminishes from the outer edge of the boundary layer to the surface. Profiles of the radiation intensity across the boundary layer are shown in figure 3 for the stronger injection $f_w=-1/\sqrt{2}$ for various values of the absorption coefficient. The solid curves correspond to solutions of equation (34) and the dashed curves to solutions of equation (35) for a surface reflectivity of 0.6. For increasing values of α, the region in which most of the absorption takes place tends to move away from the body surface ($\eta=0$).

The dashed curves in figure 3 show that the same fraction of the reflected beam is absorbed on the outward passage as that of the incident beam on the inward passage. This would be obvious from writing the formal solution of equation (35) in terms of quadratures and comparing it with equation (47). Thus for absorption coefficients of 0.5 or higher, almost none of the incident radiation finds its way back out of the boundary layer even though the surface is a good reflector.

The absorption of radiant energy within the boundary layer raises the local enthalpy level. The influence of absorption or enthalpy can be shown from solutions of the energy equation (42) which yield profiles of total enthalpy across the boundary layer. In the course of the investigation, more than 100 examples were computed; some typical enthalpy profiles are shown in figure 4 for the higher injection rate and no surface reflectivity. The enthalpy profiles for surface reflectivity conditions different from zero lie almost on top of those shown for the same values of absorption coefficient α and incident radiation intensity l_{ie}. The lower curve corresponds to either no incident radiation or no absorption. The total enthalpy level at a given distance from the surface

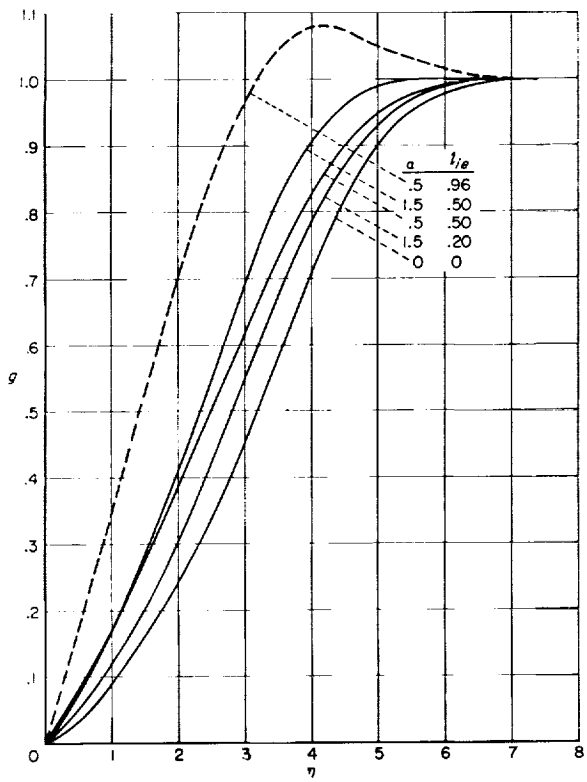

FIGURE 4.—Relative enthalpy as a function of dimensionless distance from the surface for various dimensionless gas absorption coefficients and incident radiation intensities; black surface, $f_w = 1/\sqrt{2}$, $Sc = 0.72$, $\overline{Pr} = 0.72$.

is seen to be higher if there is absorption in the boundary layer.

The dashed curve corresponds to a very large incident radiation intensity I_{ie}. It "overshoots" (i.e., $g > 1$), indicating that the local total enthalpy (and temperature if it is assumed to be roughly proportional to total enthalpy) in the boundary layer exceeds that at the outer edge of the boundary layer. In assessing the significance of this behavior, it is useful to mention two situations. For a model in the wind tunnel where the incident radiation originates in a lamp that is at a temperature much higher than the boundary-layer temperature, the overshoot condition is certainly possible. In the flight condition, the total enthalpy at the outer edge of the boundary layer will be less than that just behind the bow shock because of the emission of radiation by the shock layer. Therefore an enthalpy overshoot in the boundary layer does not necessarily mean that the enthalpy exceeds the free-stream total enthalpy. However, the question arises whether or not the cold (by comparison with the shock layer) gas assumption is violated by an enthalpy overshoot in the boundary layer. Actually, the temperature at the outer edge of the boundary layer will be less than that just behind the bow shock because of emission of radiation and chemical dissociation in the shock layer. Therefore, an overshoot in temperature in the boundary layer (corresponding to the enthalpy overshoot) could occur without violating the cold gas assumption. Thus we simply establish the fact that in the laboratory or in flight, some overshoot is possible.

However, as a convenient cut-off point in the present analysis, solutions are presented up to, but not into the overshoot region. It is worth mentioning that for injection rates lower than that of figure 4, overshoot is diminished or may vanish. Thus the region of no overshoot is extended at lower injection rates. More will be said of this in connection with a subsequent figure.

HEAT-TRANSFER RESULTS

It can be seen in figure 4 that the enthalpy gradient at the surface is increased if there is absorption in the boundary layer. This gradient is of major significance because it is proportional to the convective rate of heat transfer to the surface. It is obvious that the reduction of radiant heat transfer resulting from absorption tends to be offset by an increase of convective heat transfer. In the evaluation of this situation, it is advantageous to look at the influence of absorption coefficient, surface reflectivity, and incident radiation intensity on the enthalpy gradient at the surface. This is shown in figure 5. The solid lines correspond to black surfaces, and the dashed lines to reflecting surfaces. Two features of this figure are of particular interest. First, for a given injection rate, Prandtl number, absorption coefficient, and surface reflectivity, g'_w is linear with I_{ie}; that is,

$$g'_w = (g'_w)_{I_{ie}=0} + aI_{ie} \tag{48}$$

where $a = a(\alpha, r)$ is the slope of the straight line corresponding to a given α and r. (The linear relationship could be derived analytically, but will be omitted here.) Second, for the black surface the lines for $\alpha = 1.0$ and 1.5 lie between those of $\alpha = 0.1$ and 0.5, indicating that for a given I_{ie}, increasing α first increases the enthalpy gradient at

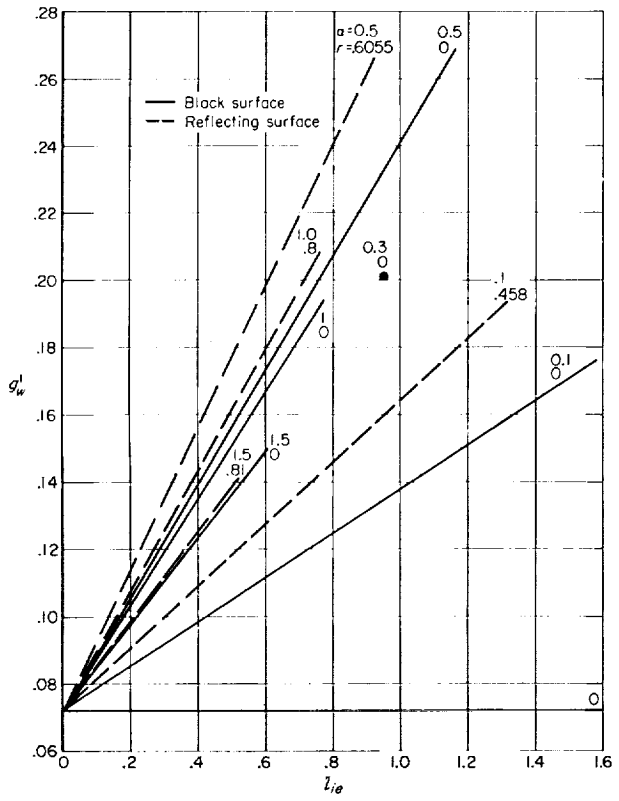

FIGURE 5.—Enthalpy gradient at the wall as a function of incident radiation intensity for various values of dimensionless gas absorption coefficient and surface reflectivity; $f_w=-1/\sqrt{2}$, $Sc=0.72$, $\overline{Pr}=0.72$.

the surface, but for higher values of α, the surface enthalpy gradient tends to diminish toward the no absorption value. Physically, for a given incident radiation intensity, increasing the absorption coefficient from zero will raise the local enthalpy near the wall by absorption of radiant energy. However, a coefficient is reached above which less radiant energy is absorbed near the wall, thereby allowing the enthalpy and its gradient at the wall to diminish. The single point for $\alpha=0.3$ shown in figure 5 was computed to see if it lies between the $\alpha=0.1$ and 0.5 lines, which it does.

The gradients indicated by the dashed lines in figure 5 corresponding to reflecting surfaces lie, as would be expected, above the black surface lines for the same α.

So far, it has been shown that in shielding the surface from radiant energy, the convective heat transfer to the surface is increased. It now must be shown whether or not a net saving in heat

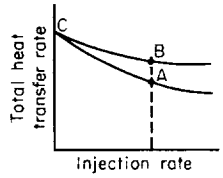

Sketch (b)

transfer results from injection of an absorbing gas. Injecting a nonabsorbing gas into the boundary layer will diminish the total heat-transfer rate to the surface by reducing the convective part of the heat transfer rate, as for example is diagrammed by the upper curve in sketch (b). The injection of an absorbing gas might be expected to diminish the total heat-transfer rate even further (as shown by the lower curve in sketch (b)). A comparison will be made of the total heat-transfer rate with injection of an absorbing and a nonabsorbing gas at the same rate (A will be compared with B). The total heat-transfer rate to a surface through which an absorbing gas is injected is expressed by equation (12) which consists of convection, diffusion, and radiation terms. By transformation and rearrangement of terms, equation (12) can be expressed as

$$\frac{q_{\text{with absorption}}}{j_e\sqrt{(n+1)\beta\rho_e\mu_e}}=\sqrt{C}\left[\frac{-g'_w}{\overline{Pr}}+(r-1)l_{iw}\right] \tag{49}$$

Similarly, the dimensionless total heat-transfer rate to a surface through which a nonabsorbing gas is injected at the same rate is

$$\frac{q_{\text{no absorption}}}{j_e\sqrt{(n+1)\beta\rho_e\mu_e}}=\sqrt{C_{\alpha=0}}\left[-\left(\frac{g'_w}{\overline{Pr}}\right)_{\alpha=0}+(r-1)l_{iw}\right] \tag{50}$$

The denominators of the left-hand sides of equations (49) and (50) contain only exterior flow variables which may be calculated for a given flight condition. The $\sqrt{C}$ is retained on the right-hand sides because it is influenced by a wall condition not calculable from a flight condition. In reference 7, it is evaluated as

$$C=\left(\frac{\rho_w\mu_w}{\rho_e\mu_e}\right)^b \tag{51}$$

where b is some power determined empirically for mixtures that do not contain a light-gas component. Thus for injection of different gases

(absorbing and nonabsorbing), the value of C may differ for a given flight condition because $\rho_w\mu_w$ will vary. Reference 8 shows that for mixtures of atomic and molecular oxygen and nitrogen containing CO and CN, the exponent b is 0.2. But we are concerned with the half power of b in equations (49) and (50). For a given flight condition, if b is a small fractional power (0.2, for example) $\rho_w\mu_w$ can differ from $(\rho_w\mu_w)_{\alpha=0}$ by a substantial amount (almost a factor of 3 either way) and yet $\sqrt{C}$ differs from $\sqrt{C_{\alpha=0}}$ by only a small amount (about 10 percent). We will subsequently make use of the fact that for b equal to a small fractional power, $\sqrt{C/C_{\alpha=0}}\approx 1$.

Comparing the heat-transfer rate with absorption to that without absorption for a given injection rate by use of equations (49) and (50) yields

$$\frac{q_{\text{ with absorption}}}{q_{\text{ no absorption}}}=\sqrt{\frac{C}{C_{\alpha=0}}}\left[\frac{(g'_w/\overline{Pr})+(1-r)l_{iw}}{(g'_w/\overline{Pr})_{\alpha=0}+(1-r)l_{ie}}\right] \quad (52)$$

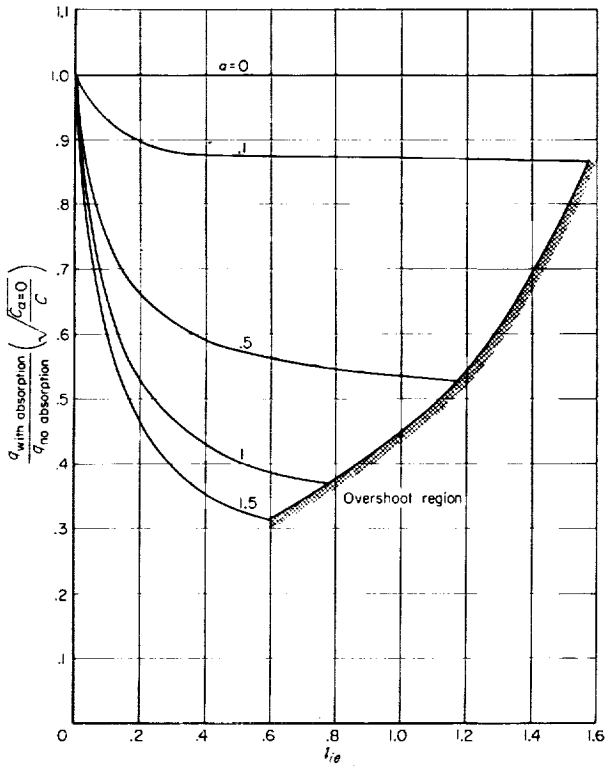

FIGURE 6.- Ratio of heat transfer with injected absorbing gas to that with injected nonabsorbing gas as a function of incident radiation intensity for several values of dimensionless gas absorption coefficient; $f_w=-1/\sqrt{2}$, black surface. $Sc=0.72$, $\overline{Pr}=0.72$.

The comparison is shown in figure 6 for the higher injection rate (corresponding to $f_w=-1/\sqrt{2}$). If $\sqrt{C_{\alpha=0}/C}$ is assumed to be of the order unity, the figure shows that for the black surface it is advantageous to inject an absorbing gas. The effectiveness of this method of shielding against excessive heating increases with increasing absorption coefficient and incident radiation intensity. For $\alpha=1.5$, and $l_{ie}=0.5$, the total heat-transfer rate at the surface is diminished by approximately 2/3. The shaded region to the right of these curves corresponds to the enthalpy overshoot condition. It should be pointed out that for the lower injection rate, overshoot is much less severe and the no overshoot region would be extended to the right in figure 6. In particular, for $\alpha=0.5$, diminishing the injection rate $(f_w=-1/\sqrt{2})$ by half (to $f_w=-1/2\sqrt{2}$) extends the overshoot limit from $l_{ie}\approx 1.17$ to $l_{ie}\approx 1.95$.

It is worth noting that a combination of equations (52), (48), and (47) yields an expression for the curves of figure 6 (although the curves were not obtained by this expression). It is

$$\frac{q_{\text{ with absorption}}}{q_{\text{ no absorption}}}=\sqrt{\frac{C}{C_{\alpha=0}}}\left\{\frac{l_{ie}\left[\frac{a(\alpha,r)}{\overline{Pr}}+(1-r)e^{-\alpha\int_0^\infty W d\eta}\right]+\left(\frac{g'_w}{\overline{Pr}}\right)_{l_{ie}=0}}{\left(\frac{g'_w}{\overline{Pr}}\right)_{\alpha=0}+(1-r)l_{ie}}\right\} \quad (53)$$

Using, for example, the value 2.73 for the integral (mentioned previously in connection with eq. (47)), 0.72 for $\overline{Pr}$, 0.0714 for $(g'_w)_{l_{ie}=0}$, and from figure 5, the value $a=0.160$ corresponding to $\alpha=1$ and $r=0$ yields the simple relationship

$$\frac{q_{\text{ with absorption}}}{q_{\text{ no absorption}}}=\sqrt{\frac{C}{C_{\alpha=0}}}\left(\frac{0.0992+0.287\ l_{ie}}{0.0992+l_{ie}}\right) \quad (54)$$

which can be used to describe the appropriate curve in figure 6.

Before leaving the discussion of the black surface, it is also of interest to compare the total heat-transfer rate with injection of an absorbing gas to the total heat-transfer rate without injection (A vs. C in sketch (b)). The dimensionless total heat-transfer rate at the surface without injection is

$$\frac{q_{\text{no injection}}}{i_e\sqrt{(n+1)\beta\rho_e\mu_e}}=\sqrt{C_{f_w=0}}\left[-\left(\frac{g'_w}{\overline{Pr}}\right)_{f_w=0}+(r-1)l_{ie}\right] \tag{55}$$

The ratio of equation (49) to (55) is [1]

$$\frac{q_{\text{with absorption}}}{q_{\text{no injection}}}=\sqrt{\frac{C}{C_{f_w=0}}}\left[\frac{\frac{g'_w}{\overline{Pr}}+(1-r)l_{iw}}{\left(\frac{g'_w}{\overline{Pr}}\right)_{f_w=0}+(1-r)l_{ie}}\right] \tag{56}$$

The comparison is shown in figure 7. The higher injection rate corresponding to $f_w=-1/\sqrt{2}$ is used for the absorption condition in the numerator of equation (56). Examination of the figure shows

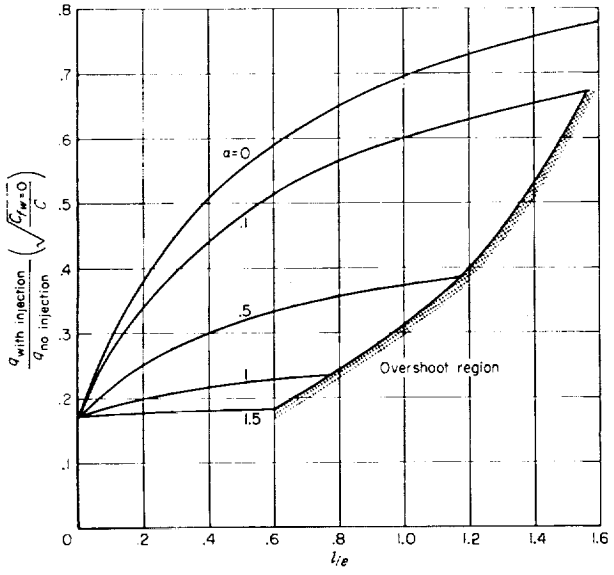

FIGURE 7.—Ratio of heat transfer with injected absorbing gas to that without injection as a function of incident radiation intensity for several values of dimensionless gas absorption coefficient; $f_w=-1/\sqrt{2}$, black surface, $Sc=0.72$, $\overline{Pr}=0.72$.

first of all that for cases involving black surfaces, it is advantageous to inject a gas whether it absorbs radiation or not. As seen before, the heat-transfer rate is diminished more by injection of an absorbing gas. However, for low levels of incident radiation intensity, a large absorption coefficient is not much more effective than a small absorption coefficient in reducing the total heat-transfer rate. Again, for large values of incident radiation intensity, large absorption coefficients are very advantageous. In particular, for $\alpha=1.5$, the heat-transfer rate is only 1/5 that for no injection for all values of incident radiation intensity, and less than 1/2 that for injecting a nonabsorbing gas if $l_{ie}=0.5$.

Leaving the black surface condition, attention is now turned to the partially reflecting surface. It has already been mentioned that it is not desirable to inject an absorbing gas to shield a totally reflecting surface because it would increase the total heat transfer by raising the convective heating rate. Also, the concept has been introduced of a break even reflectivity condition between the totally reflecting and black surface conditions where the heat-transfer rate at the surface is the same whether the gas is absorbing or not. For surface reflectivities above this break even reflectivity, a nonabsorbing gas would provide better heat-transfer protection and below that reflectivity, an absorbing gas would provide better heat protection. It is simple to show from the preceding development that for a given injection rate, the break even surface reflectivity is a function only of the absorption coefficient of the opaque gas (if $\sqrt{C_{\alpha=0}}\approx\sqrt{C}$). This is done by setting the left-hand side of equation (52) to unity and then combining it with equations (47) and (48). It is noted that the values used for $(\overline{Pr})_{\alpha=0}$ and $\overline{Pr}$ are the same and thus $(g'_w)_{\alpha=0}=(g'_w)_{l_{ie}=0}$. The result is

$$r^*=1-\frac{a(\alpha,r)}{\overline{Pr}\left(1-e^{-\alpha\int_0^\infty W\,d\eta}\right)} \tag{57}$$

The integral in the denominator has only one value for a given f_w and Sc. Thus with Sc fixed, and for a given injection rate, the break even reflectivity is a function of the foreign gas absorption coefficient alone. This derived result was verified by numerical solutions of the differential equations, and the results presented below are obtained from those solutions.

Figure 8 shows the ratio of total heat-transfer rate with injection of an absorbing gas to that with injection of a nonabsorbing gas at the same rate as a function of l_{ie} for various surface reflectivities. The curves all correspond to $\alpha=1$ and to the higher injection rate $(f_w=1/\sqrt{2})$. The bottom curve is for the black surface, and the top curve

[1] Equations (56), (48), and (47) could be combined to obtain the heat-transfer ratio between injection with absorption and the no injection case, corresponding to equation (53).

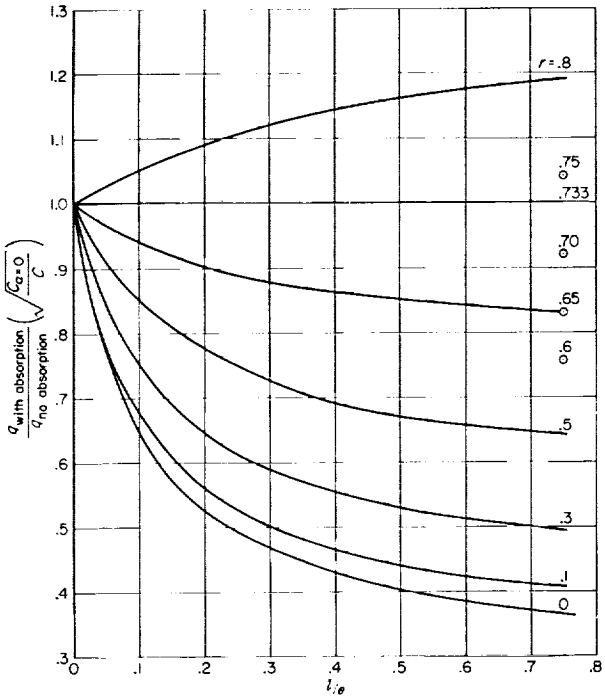

FIGURE 8.—Ratio of heat transfer with injected absorbing gas to that with injected nonabsorbing gas as a function of incident radiation intensity for various values of surface reflectivity; $f_w=-1/\sqrt{2}$; $\alpha=1$, $Sc=0.72$, $\overline{Pr}=0.72$.

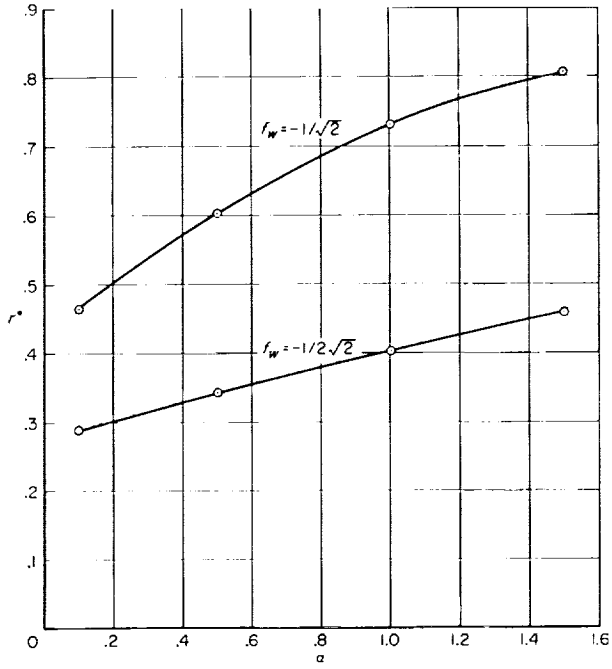

FIGURE 9. Breakeven reflectivity as a function of dimensionless gas absorption coefficient for two injection rates; $Sc=0.72$, $\overline{Pr}=0.72$.

is for a reflectivity of 0.8. The heat-transfer comparison is unity for $r=0.733$ and is seen to be independent of incident radiation intensity l_{ie}. Thus the break even reflectivity condition for $\alpha=1$ is $r=0.733$ if $\sqrt{C_{\alpha=0}/C}\approx 1$ for the higher injection rate.

The break even reflectivity conditions for other values of α were obtained in a similar manner and are shown in figure 9. In general, the break even surface reflectivity increases with increasing foreign gas absorptivity α. For surface reflectivities above the line corresponding to a given injection rate, heat protection is best afforded by injection of a transparent gas, and below the curve, by injection of an absorbing gas. The figure shows that the break even reflectivity is diminished roughly 40 to 45 percent by a 50 percent reduction of the injection rate.

In all the results presented in this paper, $\overline{Pr}$ and Sc are 0.72 and Le is unity. If we assume, as in reference 7, where the convective heat transfer with mass addition and chemical reactions was studied, that the heat transfer is not greatly affected by small deviations of Le from unity, we can study some effects of variations in $\overline{Pr}$ and Sc and still omit the diffusion term in the energy equation (3b). For simplicity, it is further assumed that $\sqrt{C}\approx\sqrt{C_{\alpha=0}}$ and that the nonabsorbing injected gas used for a standard of comparison has values of $(\overline{Pr})_{\alpha=0}$ and $(Sc)_{\alpha=0}$ of 0.72. Then the results of several computed examples in which $\overline{Pr}$ and Sc were varied by about 10 percent show the following trends. An increase in $\overline{Pr}$ tends to diminish the convective heat transfer in the absorbing gas case. Also, an increase in Sc tends to diminish the radiative heat transfer in the absorbing gas mixture. Hence, the ratio of total heat transfer with injection of an absorbing gas to that with injection of a nonabsorbing gas decreases with increasing $\overline{Pr}$ and Sc. However, the ratio appears to be more affected by variations in $\overline{Pr}$ than by comparable variations in Sc. Thus the break even reflectivity is more sensitive to $\overline{Pr}$ than to Sc and increases with increasing $\overline{Pr}$.

Finally, now that the influence of the dimensionless absorption coefficient α on heat transfer and break even reflectivity has been determined, it is instructive to examine the corresponding values of the actual physical absorption coefficient K of the absorbing gas and inquire whether or

not gases with such absorption coefficients exist. The required K is dependent on the flight condition by virtue of its relationship with α (eq. (36)). For a flight speed of 31,000 feet per second at 165,000 feet altitude, and body nose radii of 1 to 10 feet, K is of the order of 10^5 to 10^7 square feet per slug for values of α ranging from 0.1 to 1.5.

Unfortunately, little is known of the absorption properties of even ordinary gases especially at conditions corresponding to the flight regime in which radiant heating is important. Measurements of Eckert and others (ref. 15, pp. 384–386) on carbon dioxide and water vapor can be interpreted to give an equivalent "gray" K for purposes of this discussion. It appears that carbon dioxide has an absorption coefficient of the order of 10 square feet per slug at ordinary pressures for temperatures up to 1600° C. The coefficient for water vapor is roughly an order of magnitude higher than that of carbon dioxide. It is interesting to find that at least three vapors have considerably higher absorption coefficients. These vapors are not inert, and their diffusion through dissociated air has not been analyzed. They are mentioned only to illustrate the existence of highly absorbing gases. They are the alkali vapors; cesium, potassium, and ribidium. All three have absorption coefficients of the order of 10^4 square feet per slug at 0° C and 1 mm Hg in the wavelength region 2000 to 3000 Å (which can be shown from ref. 16). It is interesting to note in reference 17 that the NO of dissociated air at 8000° K at 85 percent atmospheric density emits its peak radiation in this same wavelength region. There is a possibility that gases exist which have still higher absorption coefficients at higher temperatures and pressures.

CONCLUDING REMARKS

There are several interesting results of this analysis concerning the effects of injecting an absorbing gas in the stagnation region of a blunt body traveling at hypersonic speed. At a black vehicle surface, the reduction in the radiation heat-transfer rate by radiation absorption in an injected foreign gas is accompanied by an increase in the convective heat-transfer rate. However, under some circumstances, the net effect is that a saving in total heat-transfer rate (radiative plus convective) of as much as 2/3 can be achieved (at least in theory) by injecting an absorbing gas rather than a nonabsorbing gas into the boundary layer.

For a weakly reflecting vehicle surface, the total heat transfer is reduced by injecting an absorbing gas into the boundary layer. This thermal protection diminishes to zero as the surface reflectivity increases up to the break even reflectivity condition. For surface reflectivity above the break even condition, injection of a transparent gas offers better heat protection, and below that reflectivity, an absorbing gas offers better heat protection.

In the examples studied, the break even surface reflectivity is shown to be a function of the absorption coefficient of the foreign gas and to increase with increasing absorption coefficient. The break even reflectivity is quite high, ranging from about 0.5 to 0.8 for a high injection rate and is almost proportionally lower for the lower injection rate considered, ranging from about 0.29 to 0.46. Thus for many oxidized or nonmetallic surfaces, the reflectivity would be below the break even condition and it would be advantageous to inject an absorbing gas.

The absorbing gas must have a high absorption coefficient (several orders of magnitude higher than water vapor) to effectively reduce the total heat-transfer rate to the stagnation region. It would be desirable to determine the absorption coefficient and other physical properties ($\overline{Pr}$, Sc, Le) of various gases. This should be done not only to find those that are useful absorbers but also to find those that are transparent for use with highly reflecting surfaces.

AMES RESEARCH CENTER
NATIONAL AERONAUTICS AND SPACE ADMINISTRATION
MOFFET FIELD, CALIF., *Dec. 6, 1960*

REFERENCES

1. Kivel, Bennett: Radiation From Hot Air and Stagnation Heating. AVCO Research Lab., Res. Note 165, Oct. 1959.
2. Howe, John Thomas, and Mersman, William A.: Solutions of the Laminar Compressible Boundary Layer Equations With Transpiration Which are Applicable to the Stagnation Regions of Axisymmetric Blunt Bodies. NASA TN D-12, 1959.
3. Howe, John Thomas: Radiation Shielding of the Stagnation Region by Transpiration of an Opaque Gas. NASA TN D-329, 1960.
4. Tellep, D. M., and Edwards, D. K.: General Research Flight Sciences. Vol. 1, pt. I, Jan. 1959–Jan. 1960. Radiant-Energy Transfer in Gaseous Flows. Lockheed Aircraft Corp., LMSD 288139, Paper No. 2.
5. Chandrasekhar, S.: Radiative Transfer. Oxford, Clarendon Press, 1950.
6. Jakob, Max: Heat Transfer. Vol. 1, J. Wiley and Sons, Inc., 1949.
7. Lees, Lester: Convective Heat Transfer With Mass Addition and Chemical Reactions. Paper presented at Third Combustion and Propulsion Colloquium, AGARD, NATO Palermo, Sicily, 1958. Pargamon Press. (Calif. Inst. Of Tech., Pub. 451)
8. Kourganoft, V.: Basic Methods in Transfer Problems. Oxford, Clarendon Fress, 1952.
9. Levy, Solomon: Effect of Large Temperature Changes (Including Viscous Heating) Upon Laminar Boundary Layers With Variable Free-Stream Velocity. Jour. Aero. Sci., vol. 21, no. 7, July 1954, pp. 459–474.
10. Chapman, Dean R., and Rubesin, Morris W.: Temperature and Velocity Profiles in the Compressible Laminar Boundary Layer With Arbitrary Distribution of Surface Temperature. Jour. Aero. Sci., vol. 16, no. 9, Sept. 1949, pp. 547–565.
11. Lees, Lester: Laminar Heat Transfer Over Blunt-Nosed Bodies at Hypersonic Flight Speeds. Jet Propulsion, vol. 26, no. 4, Apr. 1956.
12. Chung, Paul M.: Shielding Stagnation Surfaces of Finite Catalytic Activity by Air Injection in Hypersonic Flight. NASA TN D-27, 1959.
13. Emmons, H. W., and Leigh, D.: Tabulation of the Blasius Function With Blowing and Suction. Combustion Aerodynamics Lab., Interim Tech. Rep. 9. Harvard Univ., Nov. 1953.
14. Hildebrand, F. B.: Introduction to Numerical Analysis. McGraw-Hill Book Co., 1956.
15. Eckert, Ernest R., and Drake, Robert M., Jr.: Heat and Mass Transfer. Second Edition, McGraw-Hill Book Co., Inc., 1959.
16. Cobine, James D.: Gaseous Conductors, Theory and Engineering Applications. Dover Pub. Inc., 1958, page 89.
17. Kivel, B., and Bailey, K.: Tables of Radiation From High Temperature Air. AVCO Research Lab., Res. Rep. 21, Dec. 1957.

U.S. GOVERNMENT PRINTING OFFICE: 1961